

# Iteratively-Reweighted Local Model Fitting Method for Adaptive and Accurate Single-Shot Surface Profiling

Nozomi Kurihara

Tokyo Institute of Technology

2-12-1 O-okayama, Meguro-ku, Tokyo, 152-8552, Japan.

kurihara@sg.cs.titech.ac.jp

Masashi Sugiyama

Tokyo Institute of Technology

2-12-1 O-okayama, Meguro-ku, Tokyo 152-8552, Japan.

sugi@cs.titech.ac.jp <http://sugiyama-www.cs.titech.ac.jp/~sugi>

Hidemitsu Ogawa

Toray Engineering Co., Ltd.

1-1-45 Oe, Otsu, Shiga, 520-2141, Japan.

hidemitsu-ogawa@kuramae.ne.jp

Katsuichi Kitagawa

Toray Engineering Co., Ltd.

1-1-45 Oe, Otsu, Shiga, 520-2141, Japan.

katsuichi\_kitagawa@toray-eng.co.jp

Kazuyoshi Suzuki

Toray Engineering Co., Ltd.

1-1-45 Oe, Otsu, Shiga, 520-2141, Japan.

kazuyoshi\_suzuki@toray-eng.co.jp

## Abstract

The *local model fitting (LMF)* method is one of the useful single-shot surface profiling algorithms. The measurement principle of the LMF method relies on the assumption that the target surface is locally flat. Based on this assumption, the height of the surface at each pixel is estimated from pixel values in its vicinity. Therefore, we can estimate flat areas of the target surface precisely, whereas the measurement accuracy could be degraded in areas where the assumption is violated, because of curved surface or sharp steps. In this paper, we propose to overcome this problem by weighting the contribution of the pixels according to the degree of satisfaction of the locally flat assumption. However, since we have no information on the surface profile beforehand, we iteratively estimate it and use this estimation result to determine the weights. This algorithm is named the *iteratively-reweighted LMF (IRLMF)* method. Experimental results show that the proposed algorithm, named Iteratively-Reweighted LMF (IRLMF), works excellently.

# 1 Introduction

Surface profiling using optical interferometry is useful because we can estimate the surface profile of target objects accurately and fast without damaging them. Among various methods, the *phase shift method* [1] is popular and widely used to measure surface profiles. This method uses multiple images (so it is called ‘multiple-shot’) taken by changing the relative distance between the target object and the reference mirror. Although the measurement accuracy of this method is very high, it could be degraded by disturbance such as vibration, and measurement speed is not so fast because we have to take images several times.

To overcome these problems of the multiple-shot method, surface profiling methods which only require a single image (i.e., ‘single-shot’) have been actively explored. A key idea of single-shot surface profiling is to slightly tilt the reference mirror. Such a single-shot method is robust against vibration, fast, and simple since mechanical devices such as piezo actuators are not needed. For these reasons, various single-shot methods have been developed; for example, the *Fourier transform method* [2], the *spatial phase synchronization method* [3], the *spatial phase-shift method* [4, 5], and the *local model fitting (LMF) method* [6].

In particular, the LMF method [6] was shown to be useful since its locality allows one to measure objects with sharp steps and/or covered with heterogeneous materials, which is an advantage over the Fourier transform method and the spatial phase synchronization method. Moreover, the tilting angle of the reference mirror could be arbitrary in LMF, which is an advantage over the spatial phase-shift method. Finally, the LMF method can be implemented in a simple and computationally efficient way.

The measurement principle of the LMF method relies on the assumption that the target surface is locally flat. Based on this assumption, the height at each pixel is estimated from pixel values in its vicinity by least-squares. Therefore, we can estimate flat areas of the target surface precisely, whereas the measurement accuracy could be degraded in areas where the assumption is violated, because of curved surface.

In this paper, we overcome the above limitation of LMF by weighting the contribution of pixels in the vicinity of a target pixel according to the degree of satisfaction of the locally flat assumption—more specifically, the difference of the height of the surface from the target pixel. This weighting scheme allows us to suppress the influence of pixels which strongly violate the assumption. However, since we have no information on the surface profile beforehand, we can not directly implement this idea. To cope with this problem, we iteratively estimate the surface profile and use this estimation result to determine the weights. This algorithm is named the *iteratively-reweighted LMF (IRLMF)* method. The practical usefulness of the IRLMF method is shown through experiments.

This paper is organized as follows. In Section 2, the original LMF method is briefly reviewed. In Section 3, a drawback of the LMF method is pointed out and the IRLMF algorithm is introduced. In Section 4, experimental results are reported. Finally, concluding remarks are given in Section 5.

## 2 The Local Model Fitting Algorithm

In this section, we review a single-shot surface profiling algorithm called the LMF method [6]. We tilt the reference mirror in an arbitrary angle. Then an interference pattern is modeled as

$$g(x, y) := a(x, y) + b(x, y) \cos(\phi(x, y) + 2\pi f_x x + 2\pi f_y y), \quad (1)$$

where  $a(x, y)$  and  $b(x, y)$  are the bias and the amplitude,  $\phi(x, y)$  contains information on the surface profile which we would like to extract, and  $f_x$  and  $f_y$  are the spatial carrier frequencies along the  $x$ -axis and  $y$ -axis, respectively.

We can easily show that  $g(x, y)$  is equivalently expressed as

$$g(x, y) = a(x, y) + \xi_c(x, y)\varphi_c(x, y) + \xi_s(x, y)\varphi_s(x, y),$$

where

$$\begin{aligned} \xi_c(x, y) &:= b(x, y) \cos \phi(x, y), & \varphi_c(x, y) &:= \cos(2\pi f_x x + 2\pi f_y y), \\ \xi_s(x, y) &:= b(x, y) \sin \phi(x, y), & \varphi_s(x, y) &:= -\sin(2\pi f_x x + 2\pi f_y y). \end{aligned}$$

Suppose we have samples  $\{g_i\}_{i=1}^n$  at  $\{(x_i, y_i)\}_{i=1}^n$  in the vicinity of a target point  $(x_0, y_0)$ . Our goal is to estimate  $\phi(x_0, y_0)$  from  $\{g_i\}_{i=1}^n$ . Here we make the following assumption:  $a(x, y)$ ,  $b(x, y)$ , and  $\phi(x, y)$  are constant in the vicinity of  $(x_0, y_0)$ , i.e., our local model is

$$\bar{g}(x, y) := a + \xi_c \varphi_c(x, y) + \xi_s \varphi_s(x, y), \quad (2)$$

where

$$\xi_c := b \cos \phi \quad \text{and} \quad \xi_s := b \sin \phi. \quad (3)$$

Suppose we have reasonable estimates of the spatial carrier frequencies  $f_x$  and  $f_y$ , denoted by  $\hat{f}_x$  and  $\hat{f}_y$ , respectively;  $\hat{f}_x$  and  $\hat{f}_y$  may be obtained from the image data of a flat area. Note that the spatial carrier frequencies  $f_x$  and  $f_y$  are global quantities which do not depend on the target object and are only determined by the (relative) tilting angle of the reference mirror. Then the unknown parameters in the simplified model (2) are only  $a$ ,  $\xi_c$ , and  $\xi_s$ . We determine them by solving the following least-squares problem:

$$(\hat{a}, \hat{\xi}_c, \hat{\xi}_s) := \underset{(a, \xi_c, \xi_s)}{\operatorname{argmin}} \sum_{i=1}^n \left( g_i - \bar{g}(x_i, y_i) \right)^2. \quad (4)$$

Since the above model is linear with respect to the parameters  $a$ ,  $\xi_c$  and  $\xi_s$ , we can analytically obtain the least-squares solutions  $\hat{a}$ ,  $\hat{\xi}_c$  and  $\hat{\xi}_s$  as

$$(\hat{a}, \hat{\xi}_c, \hat{\xi}_s)^\top = (\mathbf{A}^\top \mathbf{A})^{-1} \mathbf{A}^\top \mathbf{g}, \quad (5)$$

where

$$\mathbf{A} = \begin{pmatrix} 1 & \varphi_c(x_1, y_1) & \varphi_s(x_1, y_1) \\ 1 & \varphi_c(x_2, y_2) & \varphi_s(x_2, y_2) \\ \vdots & \vdots & \vdots \\ 1 & \varphi_c(x_n, y_n) & \varphi_s(x_n, y_n) \end{pmatrix}, \quad \mathbf{g} = \begin{pmatrix} g_1 \\ g_2 \\ \vdots \\ g_n \end{pmatrix}.$$

Given  $\hat{\xi}_c$  and  $\hat{\xi}_s$ , we can obtain an estimate  $\hat{\phi}$  of the surface profile at  $(x_0, y_0)$  by

$$\hat{\phi} := \arctan\left(\frac{\hat{\xi}_s}{\hat{\xi}_c}\right) + 2m\pi, \quad (6)$$

where  $m$  is an unknown integer. Note that we can determine the value of arctangent up to a  $2\pi$  range by using the signs of  $\cos \phi$  and  $\sin \phi$ . Since  $b$  is always positive, the signs of  $\cos \phi$  and  $\sin \phi$  could be estimated by the signs of  $\hat{\xi}_c$  and  $\hat{\xi}_s$ , respectively (cf. Equation (3)).  $m$  may be determined by a phase-unwrapping algorithm [9].

### 3 The Iteratively-Reweighted LMF Algorithm

In this section, we first point out a drawback of the LMF method, and then propose a new algorithm which can solve it.

#### 3.1 Drawback of the LMF Method

The key idea of the LMF method was that  $a(x, y)$ ,  $b(x, y)$ , and  $\phi(x, y)$  are assumed to be constant in the vicinity of  $(x_0, y_0)$ , which enabled us to estimate unknown parameters in the model. Although  $a(x, y)$  and  $b(x, y)$  would be almost locally constant,  $\phi(x, y)$  is far from constant when the local area is not flat. Then some measurement error would be incurred. We first demonstrate this problem through computer simulations.

We prepared two target surfaces: a sharp bump and a sphere illustrated in Figure 1(a) and Figure 2(a), respectively. The number of pixels is  $100 \times 100 = 10000$ . We generated observed interference patterns by Equation (1), and added Gaussian noise with mean 0 and standard deviation 0.1. Here the signal-to-noise ratio (the standard deviation of the signal  $g(x, y)$  divided by that of the noise) of the bump and sphere are 50.02 and 50.00, respectively. Figures 1(b) and 2(b) depict observed images  $g(x, y)$ , while Figures 1(c) and 2(c) depict their one-dimensional intercepts at  $y = 50$ . In the following simulations, we evaluate the accuracy of estimation results by root mean squared error (RMSE).

We estimated surface profiles by the LMF method for the vicinity window size:  $17 \times 17$  and  $5 \times 5$ . Recovered surfaces and their one-dimensional intercepts at  $y = 50$  are illustrated in Figures 1(d)(e)(g)(h) and 2(d)(e)(g)(h), respectively.

In the bump case, if we set the window size large, a lot of samples can be used for estimation. Then the influence of noise is well suppressed, and the recovered surface becomes smooth (see Figures 1(d)(g)). However, since the locally flat assumption is heavily violated around edges, the sharpness of the bump tends to be lost. On the other hand, if we set the

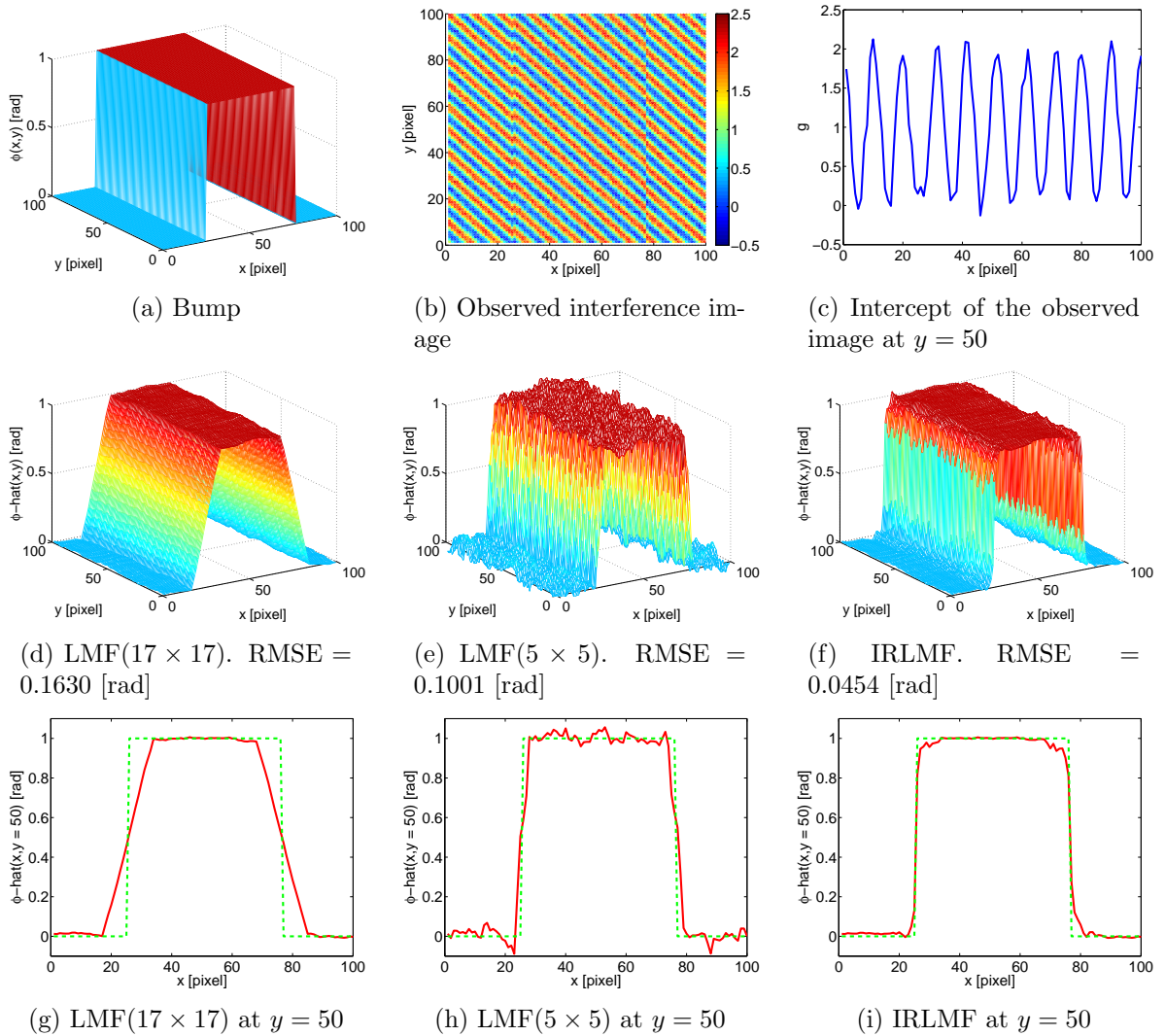


Figure 1: Simulation results for an artificial bump.

window size small, sharp edges can be successfully recovered (see Figures 1(e)(h)). However, flat or smooth areas become rather noisy because the number of samples used for estimation is small. A similar tendency can be also observed in the sphere case (see Figures 2(d)(e)(g)(h)).

### 3.2 The Iteratively-Reweighted LMF Algorithm

The above simulation results show that the window size control the trade-off between sharpness and smoothness. However, it is not possible to achieve both as long as the window size is common to all pixels globally. It seems more appropriate to determine the window shape and size *adaptively* according to the local surface profile, i.e., the pixels whose height of the surface is considerably different from the target height should be excluded from the vicinity.

To confirm the validity of this idea, we carried out the simulation of the LMF method

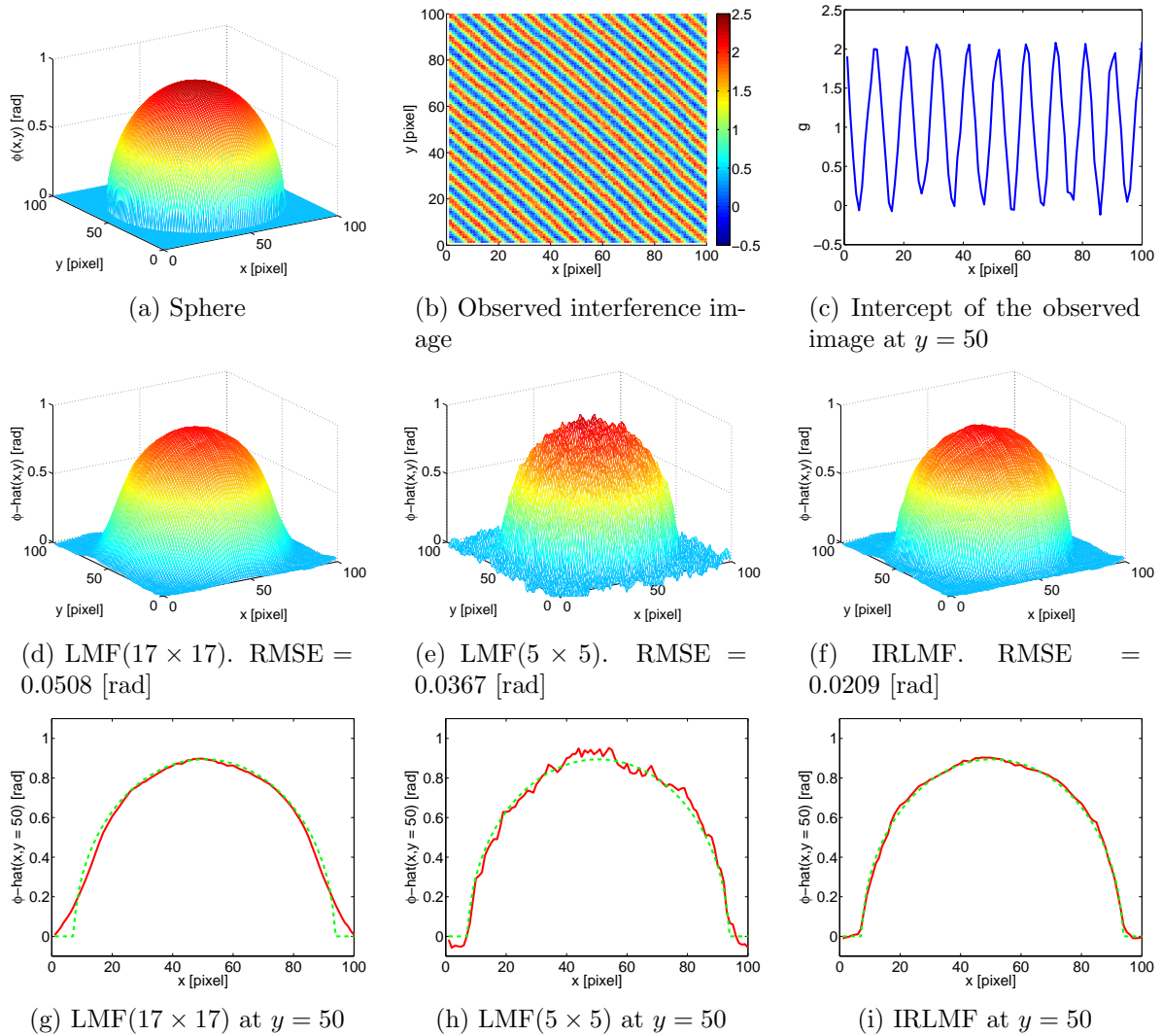


Figure 2: Simulation results for an artificial sphere.

with ‘ideal’ window shape and size, under the hypothetical setup that we know the true surface of objects. Here the experimental setting is the same as Section 3.1. The results are illustrated in Figures 3(a)–(c) and 4(a)–(c).

We first determined the window size as  $17 \times 17$ , and excluded pixels whose difference of the phase  $\phi$  (recall that it is proportion to the height of the surface as mentioned in Section 2) from the target pixel is larger than 0.03. Figures 3(a) and 4(a) depict the determined window shape. In these figures, the central point of each window expresses the target pixel, and deep-colored points are pixels included as vicinity and light-colored points are excluded pixels. For example, in the bump case, each window is determined not to stride over edges.

Recovered surfaces are illustrated in Figures 3(b) and 4(b), while their one-dimensional intercepts at  $y = 50$  are illustrated in Figures 3(c) and 4(c). We can see that the recovered surfaces become more accurate than those shown in Section 3.1. The simulation results illus-

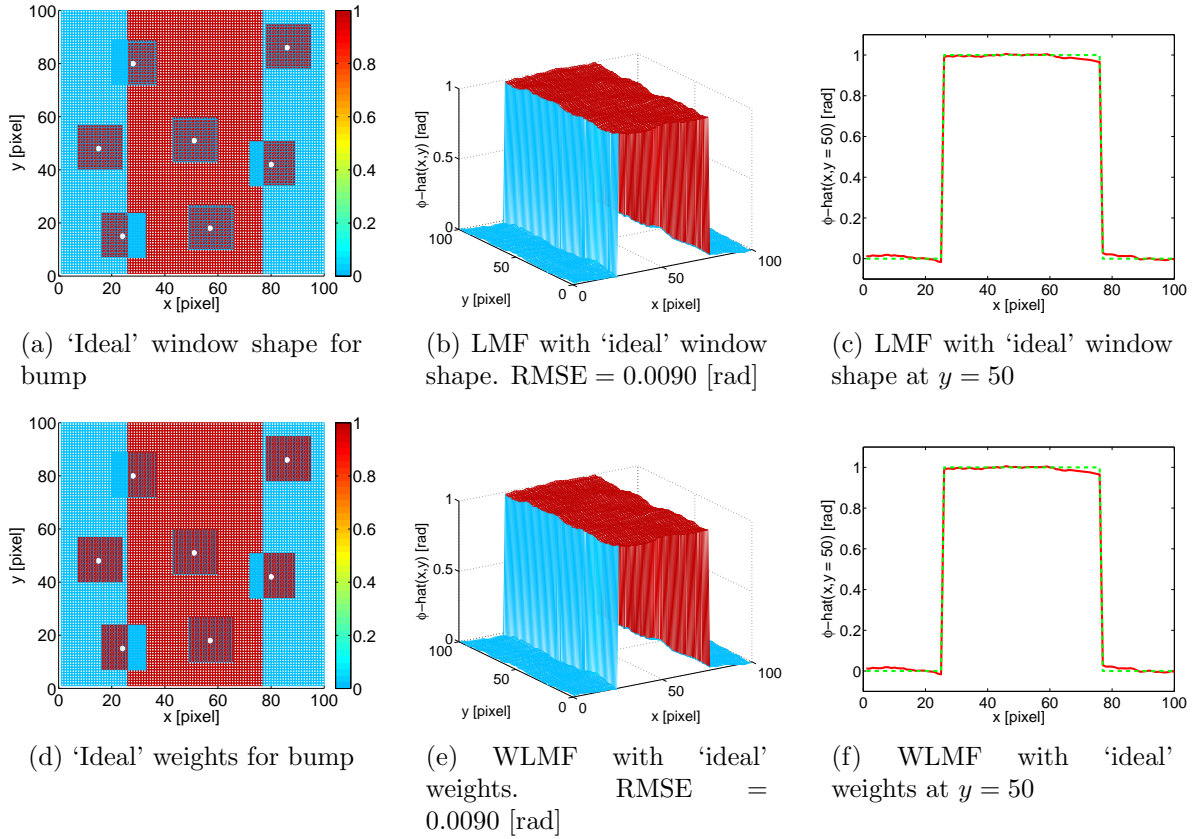


Figure 3: LMF with ‘ideal’ window shape and WLMF with ‘ideal’ weights for bump.

trate that the measurement accuracy of the LMF method can be improved by determining the window shape adaptively according to the local surface profile.

However, when the local region is not really flat, the above procedure may result in a very small window, yielding less accurate estimation. To cope with this problem, we propose to *weight* the influence of pixels in the window according to their difference of the height from the target pixel. Thus, we use a “soft” window to fully make use of the information brought by surrounding pixels. More specifically, we replace Equation (4) by weighted least-squares with weights  $\{w_i\}_{i=1}^n$ :

$$(\tilde{a}, \tilde{\xi}_c, \tilde{\xi}_s) := \operatorname{argmin}_{(a, \xi_c, \xi_s)} \left[ \sum_{i=1}^n w_i (g_i - \bar{g}(x_i, y_i))^2 \right]. \quad (7)$$

We can still analytically obtain the weighted least-squares solutions  $\tilde{a}$ ,  $\tilde{\xi}_c$  and  $\tilde{\xi}_s$  as

$$(\tilde{a}, \tilde{\xi}_c, \tilde{\xi}_s)^\top = (\mathbf{A}^\top \mathbf{W} \mathbf{A})^{-1} \mathbf{A}^\top \mathbf{W} \mathbf{g}, \quad (8)$$

where  $\mathbf{W}$  is the  $n$ -dimensional diagonal matrix whose diagonal elements are  $\{w_i\}_{i=1}^n$ :

$$\mathbf{W} = \operatorname{diag}(w_1, w_2, \dots, w_n). \quad (9)$$

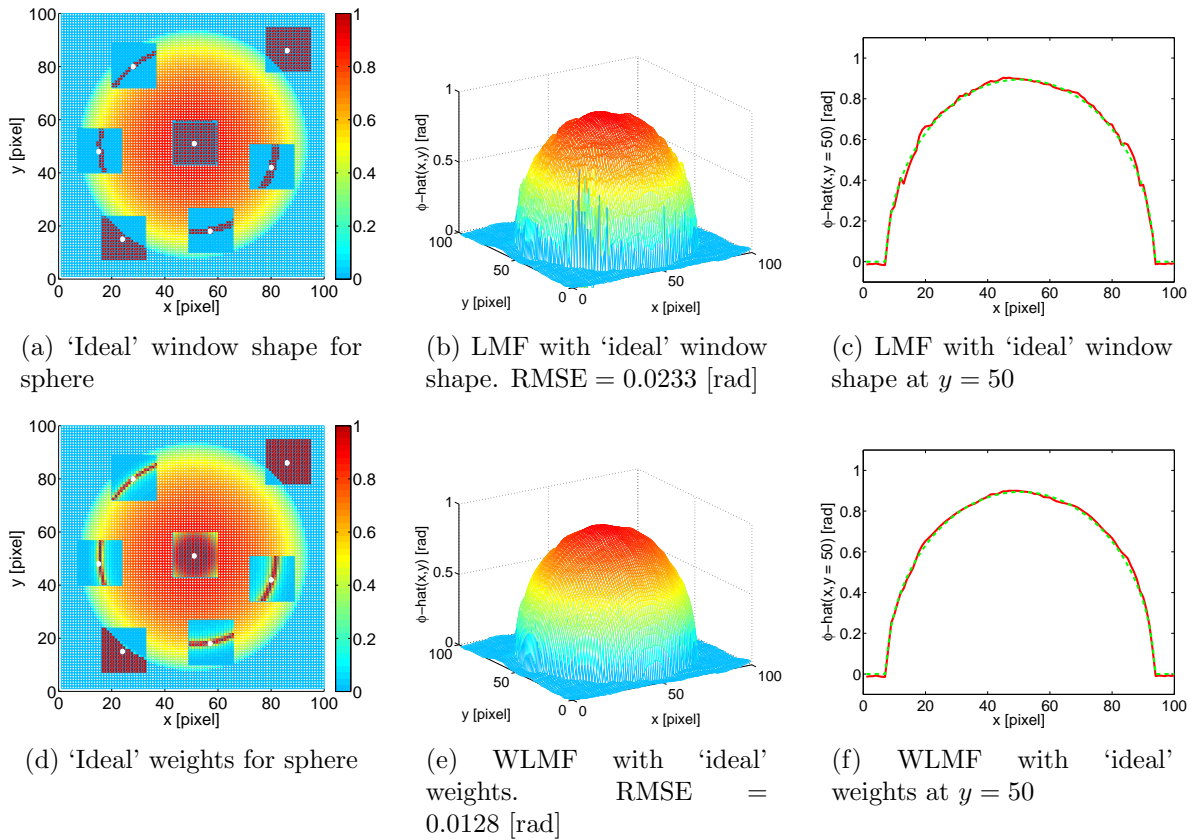


Figure 4: LMF with ‘ideal’ window shape and WLMF with ‘ideal’ weights for sphere.

We call this algorithm the *weighted LMF (WLMF)* method.

Figures 3(d)–(f) and 4(d)–(f) show the simulation result of the WLMF method (this is obtained under the ‘ideal’ setup). We determined  $w_i$ , which is the weight at  $(x_i, y_i)$ , by the following equation:

$$w_i = c \left( (\phi(x_0, y_0) - \phi(x_i, y_i))^2 + c \right)^{-1}, \quad (10)$$

where  $c$  is a constant to avoid divergence of the weight  $w_i$ . We set it to  $c = 0.001$ . Figures 3(d) and 4(d) depict the determined weights. In these figures, each square and central point expresses the window and the target pixel, respectively. Colors in each square illustrate the weight values. Recovered surfaces are illustrated in Figures 3(e) and 4(e), while their one-dimensional intercepts at  $y = 50$  are illustrated in Figures 3(f) and 4(f). We can see that the influence of noise is better suppressed and the recovered surface becomes smoother than those of the “hard”-windowed counterpart, especially in the sphere case. The results show that weighting (“soft”-windowing) is more sensible than thresholding (“hard”-windowing).

However, since we have no information on the true surface profile, the above “ideal” procedure can not be directly implemented. To cope with this problem, we propose the following iterative algorithm: first we initialize the weights uniformly and execute the (W)LMF method. Next we update the weights by using the estimation result. Then we execute the



WLMF method again based on the current weights, and update the weights by using the new estimation result. We iterate these height-estimating step and weight-updating step until convergence, and we obtain the final estimation result.

We call this algorithm the *iteratively-reweighted LMF (IRLMF)* method. A pseudo-code of IRLMF algorithm is summarized below.

1. Initialize the weights uniformly ( $w_1 = w_2 = \dots = w_n = 1$ ).
2. Estimate the surface profile by executing the WLMF method based on the current weights.
3. Update the weights based on the estimated surface profile.
4. Repeat 2 and 3 until convergence.

We note that in preliminary experiments, we empirically found that repeating the above IRLMF iteration only once (i.e., after the initial LMF estimation, weights are updated and WLMF is performed only once) is sufficient for improving the estimation accuracy. For this reason, the number of repetition is set to one in the experiments below. This brings another practical advantage that the computation cost can be saved.

### 3.3 Computer Simulations of the IRLMF Method

We demonstrate the behavior of the IRLMF method through computer simulations. Here the experimental setting is the same as Section 3.1. We used the estimation result by the LMF method with window size  $17 \times 17$  (see Figures 1(d)(c) and 2(d)(c)) as an initial solution, and weights are determined as

$$w_i = c \left( (\hat{\phi}(x_0, y_0) - \hat{\phi}(x_i, y_i))^2 + c \right)^{-1}, \quad (11)$$

where  $\hat{\phi}$  is an obtained estimate of the phase  $\phi$  and  $c = 0.001$ . Then we estimated the surface profile by the WLMF method. Estimation results are evaluated by RMSE.

Recovered surfaces are illustrated in Figures 1(f) and 2(f), while their one-dimensional intercepts at  $y = 50$  are illustrated in Figures 1(i) and 2(i). We can see that the measurement error is considerably reduced and the influence of noise is well suppressed. Figures 5(a) and 5(b) illustrate the weights determined by Equation (11) at the first iteration, which are reasonably adjusted to the local surface profile.

## 4 Actual Experiments

In this section, we report the experimental result of actual measurement.

We obtained interference images by using the optical surface profiler *SP-500* by Toray Engineering Co., Ltd.<sup>1</sup>, which allows a full-field measurement of 512 by 480 pixels (the actual

<sup>1</sup>See '<http://www.cable-net.ne.jp/corp/torayins/SP-500.html>' for details.

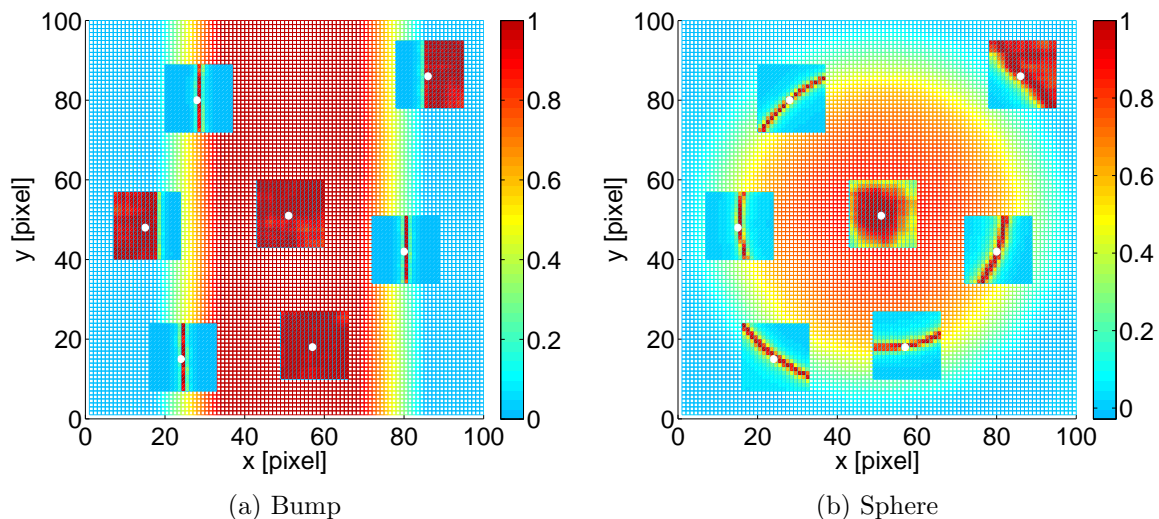


Figure 5: Weights at the first iteration.

size is  $0.80 \text{ [mm]} \times 0.72 \text{ [mm]}$ ). Each pixel takes an integer value from 0 to 255 (i.e., 8-bit intensity). The wavelength of the light source (here we used a narrow-band optical filter) is  $603 \text{ [nm]}$ .

Figure 6(a) illustrates the surface profile of the target object. The height of the bump is  $67.7 \pm 1.2 \text{ [nm]}$  (which corresponds to  $1.41 \text{ [rad]}$  in phase). The number of pixels in the measured area is  $120 \times 120 = 14400$  (i.e.,  $0.19 \text{ [mm]} \times 0.18 \text{ [mm]}$ ). Figure 6(b) depicts the observed image, and Figure 6(c) depicts the one-dimensional intercept at  $y = 60$ .

We compared the following three methods: LMF with window size  $5 \times 5$ , LMF with window size  $17 \times 17$ , and IRLMF. In the IRLMF method, the vicinity size was set to  $17 \times 17$  and weights were updated in the same way as Section 3.3. The number of iteration was set to one.

Estimation results are depicted in Figure 6. Recovered surfaces are illustrated in Figures 6(d)–(f), while their one-dimensional intercepts at  $y = 60$  are illustrated in Figures 6(g)–(i). Note that the height of the bump was accurately estimated in all methods. However, in the LMF method ( $17 \times 17$ ) (see Figures 6(d)(g)), the recovered surface became so smooth that the sharpness of the bump edge was lost. On the other hand, in the LMF method ( $5 \times 5$ ) (see Figures 6(e)(h)), although sharp edges were well recovered, flat areas became rather noisy. In contrast, in the IRLMF method (see Figures 6(f)(i)), both recovery of the sharpness of the bump edge and suppression of the noise in the flat areas are successfully achieved. Figure 7 illustrates the weights at the first iteration in the IRLMF method, which reasonably reflect the local surface profile. The computation time of the LMF ( $5 \times 5$ ), the LMF ( $17 \times 17$ ) and the IRLMF methods was  $1.84 \text{ [sec]}$ ,  $2.30 \text{ [sec]}$  and  $5.09 \text{ [sec]}$  with our implementation using Matlab, respectively. This shows that only with 2–3 times longer computation time, the proposed IRLMF can significantly improve the estimation accuracy. We also found that the computation time can be reduced by an order of magnitude by using a GPGPU, but we do not go into detail here.

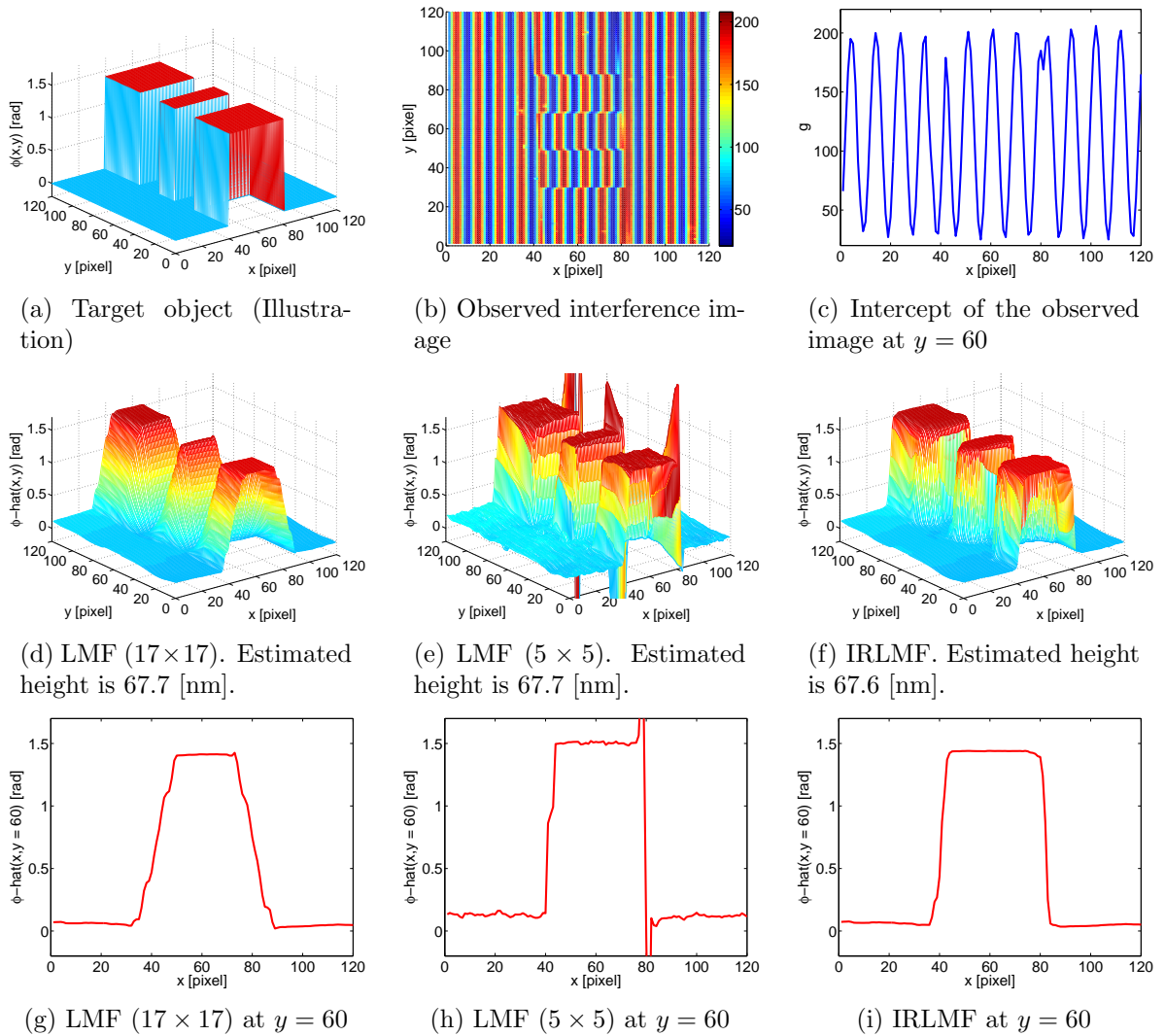


Figure 6: Actual measurement results of a real bump.

## 5 Conclusions

Single-shot surface profiling is useful in real-world situations since it is robust against external disturbance such as vibration, and the measurement system is simple. In this paper, we first reviewed a single-shot surface profiling algorithm called the LMF algorithm [6], and explained that the locally flat assumption in the LMF method enables us to estimate unknown parameters in the model analytically.

However, some measurement error can be incurred when the locally flat assumption is violated. We argued that this drawback can be avoided by determining each local window adaptively by weighting the influence of each pixel according to the degree of satisfaction of the assumption. Based on this idea, we proposed an improved single-shot surface profiling algorithm called the *iteratively-reweighted local model fitting (IRLMF)* method, which

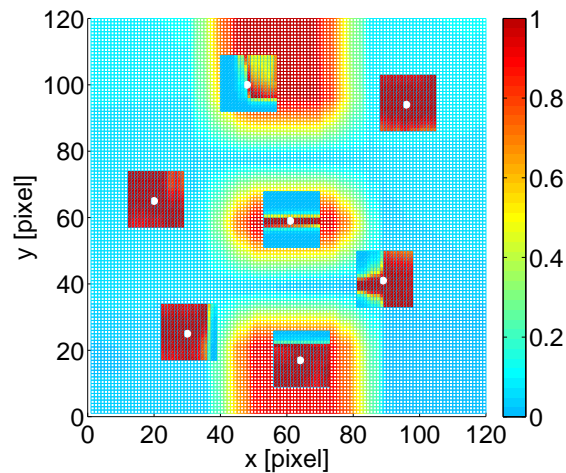


Figure 7: Weights at the first iteration (real bump).

iteratively estimates the surface profile by the *weighted local model fitting (WLMF)* method and update the weights by using the estimation result. We demonstrated high measurement accuracy of the IRLMF method through computer simulations and actual experiments.

## References

- [1] J. H. Brunning, D. R. Herriott, J. E. Gallagher, D. P. Rosenfeld, A. D. White, and D. J. Brangaccio, “Digital Wave Front Measuring Interferometer for Testing Optical Surface and Lenses,” *Applied Optics* **13**(11), 2693–2703 (1974).
- [2] M. Takeda, H. Ina, and S. Kobayashi, “Fourier-Transform Method of Fringe-Pattern Analysis for Computer-Based Topography and Interferometry,” *Journal of Optical Society of America* **72**(1), 156–160 (1982).
- [3] J. Kato, I. Yamaguchi, T. Nakamura, and S. Kuwashima, “Video-Rate Fringe Analyzer Based on Phase-Shifting Electronic Moiré Patterns,” *Applied Optics* **36**(32), 8403–8412 (1997).
- [4] D. C. Williams, N. S. Nassar, J. E. Banyard, and M. S. Virdee, “Digital Phase-Step Interferometry: A Simplified Approach,” *Optics & Laser Technology* **23**(3), 147–150 (1991).
- [5] N. Brock, J. Hayes, B. Kimbrough, J. Millerd, M. North-Morris, M. Novak, and J. C. Wyant, “Dynamic Interferometry,” in *Novel Optical Systems Design and Optimization VIII, Proceedings of SPIE*, J. M. Sasián, R. J. Koshel, and R. C. Juergens, eds., vol. 5875, pp. 1–10 (2005).
- [6] M. Sugiyama, H. Ogawa, K. Kitagawa, and K. Suzuki, “Single-Shot Surface Profiling by Local Model Fitting,” *Applied Optics* **45**(31), 7999–8005 (2006).

- [7] T. Yokota, M. Sugiyama, H. Ogawa, K. Kitagawa, and K. Suzuki, “The Interpolated Local Model Fitting Method for Accurate and Fast Single-shot Surface Profiling,” *Applied Optics* **48**(18), 3497–3508(2009).
- [8] M. Young, “Optics and Lasers: An Engineering Physics Approach,” p.73-80, Springer-Verlag, 1977
- [9] M. Takeda and T. Abe, “Phase Unwrapping by a Maximum Cross-Amplitude Spanning Tree Algorithm: A Comparative Study,” *Optical Engineering* **35**(8), 2345–2351 (1996).